Pergamon

Int. J. Solids Structures Vol. 31, No. 21, pp. 2901–2917, 1994

0020–7683/94 $7.00 + .00

0020–7683(94)00071–9

BOUNDARY ELEMENT ANALYSIS OF THICK REISSNER PLATES ON TWO-PARAMETER FOUNDATION

S. FADHIL and A. EL-ZAFRANY
Computational Mechanics Group, School of Mechanical Engineering,
Cranfield University, Cranfield, Bedford, MK43 0AL, U.K.

(*Received* 11 *January* 1994; *in revised form* 27 *April* 1994)

Abstract—This paper introduces a consistent theory for boundary element analysis of thick Reissner plates resting on a one- or two-parameter elastic foundation. Fundamental solutions and kernel functions have been derived as combinations of a group for plates on a one-parameter foundation and another group representing the effect of a second foundation parameter. Domain integral loading terms have been reduced for cases with uniformly- and linearly-distributed loadings and concentrated shear forces and bending moments. Case studies with different loading and boundary conditions have been analysed and the boundary element results have confirmed the soundness and accuracy of the developed theory.

INTRODUCTION

Due to the complexity of the actual behaviour of foundations, many idealized foundation models have appeared in the literature, the simplest of which is that of Winkler, who defined the foundation surface stress in terms of one elastic property (k) of the foundation (Selvadurai, 1979). Considering finite plate with free-edge conditions, the Winkler model results in a discontinuous deformation at the foundation surface. This problem has led to the development of more accurate foundation models, including the so-called *two-parameter models* with which the foundation surface stress is represented in terms of two independent elastic constants [see e.g. Vlasov and Leont'ev (1966); Selvadurai (1979)].

The boundary element analysis of thin plates resting on two-parameter foundations has been investigated by some researchers [see e.g. Balaš *et al.* (1984); Puttonen and Varpasuo (1986); Katsikadelis and Kallivokas (1986)]. A simplified boundary integral formulation for thick plates on a two-parameter foundation was presented by Jianguo *et al.* (1992), who ignored the effect of transverse normal stress and foundation reaction on internal moments.

This paper introduces a theory for boundary element analysis of thick plates resting on a one- or two-parameter elastic foundation, and is based upon Reissner's theory (Reissner, 1945). Fundamental solutions and kernel functions are provided as combinations of two groups, the first of which represents the case for a one-parameter foundation, and the second provides the additional effect of a second foundation parameter. This leads to an efficient inclusion of one- and two-parameter cases in one computer program. Domain integral loading terms have been reduced for cases with uniformly- and linearly-distributed loadings, and concentrated shear forces and bending moments. Boundary element analysis of plates with arbitrary shapes and different boundary conditions is discussed.

BASIC GOVERNING EQUATIONS

Consider a plate with a uniform thickness h and a midplane represented by a domain Ω in the x–y plane, as shown in Fig. 1. The upper surface of the plate ($z = -h/2$) is subjected to a distributed loading with intensity $q_U = q(x, y)$, and its lower surface ($z = h/2$) is resting on a two-parameter elastic foundation and subjected, therefore, to a stress defined as follows:

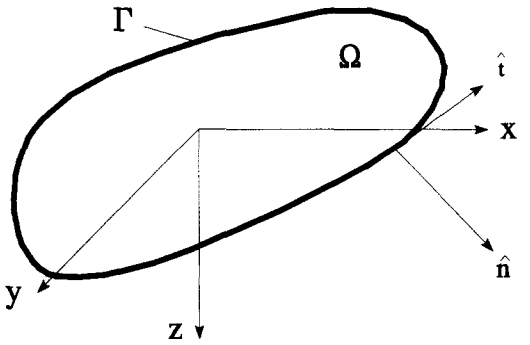

Fig. 1. Plate midplane.

$$q_L = -kw + G_p \nabla^2 w, \tag{1}$$

where k and G_p are the foundation elastic parameters. The Reissner theory for thick plates (Reissner, 1945) can be employed with the following equation for the transverse normal stress:

$$\sigma_z = \left(\frac{q_U - q_L}{2}\right) + \left(\frac{q_U + q_L}{2}\right)\left[\frac{3z}{h} - \frac{4z^3}{h^3}\right]$$

$$\equiv -\tfrac{1}{2}(q + kw - G_p \nabla^2 w) + \tfrac{1}{2}(q - kw + G_p \nabla^2 w)\left[\frac{3z}{h} - \frac{4z^3}{h^3}\right]. \tag{2}$$

Hence, the equations of bending moments per unit length can be expressed as follows:

$$M_x = D\left(\frac{\partial \theta_x}{\partial x} + \nu \frac{\partial \theta_y}{\partial y}\right) + \frac{\nu}{\lambda^2(1-\nu)}(q - kw + G_p \nabla^2 w)$$

$$M_y = D\left(\nu \frac{\partial \theta_x}{\partial x} + \frac{\partial \theta_y}{\partial y}\right) + \frac{\nu}{\lambda^2(1-\nu)}(q - kw + G_p \nabla^2 w)$$

$$M_{xy} = \tfrac{1}{2} D(1-\nu)\left(\frac{\partial \theta_x}{\partial y} + \frac{\partial \theta_y}{\partial x}\right), \tag{3}$$

where θ_x and θ_y are the average slope angles, which are related to shear forces per unit length (Q_x, Q_y) by means of the following relationship:

$$Q_\xi = \tfrac{1}{2} D(1-\nu)\lambda^2\left(\theta_\xi + \frac{\partial w}{\partial \xi}\right), \tag{4}$$

where $\xi \equiv x$ or y, D is plate flexural rigidity, ν is Poisson's ratio and $\lambda^2 = 10/h^2$.

Using an approach similar to that employed by El-Zafrany *et al.* (1994) an inverse weighted-residual expression may be obtained as follows:

$$\oint_\Gamma (M_n \theta_n^* + M_{nt} \theta_t^* + Q_n \bar{w}^*)\, d\Gamma - \oint_\Gamma (\bar{M}_n^* \theta_n + M_{nt}^* \theta_t + \bar{Q}_n^* w)\, d\Gamma$$

$$+ \iint_\Omega \left\{\theta_x\left(\frac{\partial M_x^*}{\partial x} + \frac{\partial M_{xy}^*}{\partial y} - Q_x^*\right) + \theta_y\left(\frac{\partial M_{xy}^*}{\partial x} + \frac{\partial M_y^*}{\partial y} - Q_y^*\right)\right.$$

$$\left. + w\left(\frac{\partial Q_x^*}{\partial x} + \frac{\partial Q_y^*}{\partial y} - kp^* + G_p \nabla^2 p^*\right)\right\} dx\, dy + \iint_\Omega qp^*\, dx\, dy = 0, \tag{5}$$

where θ_x^*, θ_y^* and w^* are weighting functions, Γ is the boundary of the domain Ω which represents the plate midplane,

$$p^* = w^* - \frac{\nu}{\lambda^2(1-\nu)}\left(\frac{\partial\theta_x^*}{\partial x} + \frac{\partial\theta_y^*}{\partial y}\right) \tag{6}$$

$$\bar{w}^* = w^* + \frac{2G_p p^*}{D\lambda^2(1-\nu)}, \tag{7}$$

and

$$\begin{aligned}
\bar{M}_n^* &= D\left(\frac{\partial\theta_n^*}{\partial n} + \nu\frac{\partial\theta_t^*}{\partial t}\right) + G_p p^* \\
M_{nt}^* &= \tfrac{1}{2}D(1-\nu)\left(\frac{\partial\theta_n^*}{\partial t} + \frac{\partial\theta_t^*}{\partial n}\right) \\
\bar{Q}_n^* &= \tfrac{1}{2}D\lambda^2(1-\nu)\left(\theta_n^* + \frac{\partial w^*}{\partial n}\right) + G_p\frac{\partial p^*}{\partial n}.
\end{aligned} \tag{8}$$

Notice also that

$$\begin{aligned}
&\theta_n^* = l\theta_x^* + m\theta_y^*, \qquad \theta_t^* = -m\theta_x^* + l\theta_y^* \\
&\frac{\partial}{\partial n} = l\frac{\partial}{\partial x} + m\frac{\partial}{\partial y}, \quad \frac{\partial}{\partial t} = -m\frac{\partial}{\partial x} + l\frac{\partial}{\partial y},
\end{aligned}$$

where (l, m) are the directional cosines of the outward normal to the boundary.

Equation (5) can be reduced to a boundary integral equation if θ_x^*, θ_y^* and w^* are defined as the fundamental solution to the following simultaneous partial differential equations:

$$\begin{aligned}
\frac{\partial M_x^*}{\partial x} + \frac{\partial M_{xy}^*}{\partial y} - Q_x^* &= -e_x\delta(x-x_i, y-y_i) \\
\frac{\partial M_{xy}^*}{\partial x} + \frac{\partial M_y^*}{\partial y} - Q_y^* &= -e_y\delta(x-x_i, y-y_i) \\
\frac{\partial Q_x^*}{\partial x} + \frac{\partial Q_y^*}{\partial y} - kp^* + G_p\nabla^2 p^* &= -e_z\delta(x-x_i, y-y_i),
\end{aligned} \tag{9}$$

where e_x, e_y and e_z are arbitrary constant parameters, $\delta(x-x_i, y-y_i)$ is a two-dimensional Dirac delta function defined with respect to a source point (x_i, y_i).

FUNDAMENTAL SOLUTION PARAMETERS

The previous differential equations (9) can be reduced by means of eqns (8) to the following operational form:

$$\tfrac{1}{2}D(1-\nu)\mathbf{H}\begin{bmatrix}\theta_x^*\\ \theta_y^*\\ w^*\end{bmatrix} = -\delta(x-x_i, y-y_i)\begin{bmatrix}e_x\\ e_y\\ e_z\end{bmatrix}, \tag{10}$$

where

$$H_{\alpha\beta} = (\nabla^2-\lambda^2)\delta_{\alpha\beta}+\psi\frac{\partial^2}{\partial x_\alpha \partial x_\beta}$$

$$H_{\alpha 3} = -\lambda^2\frac{\partial}{\partial x_\alpha}$$

$$H_{3\beta} = (\gamma-e_1\nabla^2)\frac{\partial}{\partial x_\beta}$$

$$H_{33} = \lambda^2(e_2\nabla^2-\phi k)$$

and

$$\alpha = 1,2, \quad \beta = 1,2, \quad (x_1, x_2) \equiv (x, y)$$

$$\psi = \frac{1+\nu}{1-\nu}, \quad \phi = \frac{2}{D\lambda^2(1-\nu)}$$

$$e_1 = \frac{\nu}{1-\nu}\phi G_p, \quad e_2 = 1+\phi G_p$$

$$\gamma = \lambda^2+\frac{\nu}{1-\nu}\phi k.$$

Using a strain function technique similar to that employed by El-Zafrany *et al.* (1994), the weighting functions can be written in terms of derivatives of strain functions f_x^*, f_y^*, f_z^* as follows:

$$\begin{bmatrix}\theta_x^*\\ \theta_y^*\\ w^*\end{bmatrix} = \mathbf{H}^*\begin{bmatrix}f_x^*\\ f_y^*\\ f_z^*\end{bmatrix} \equiv \mathbf{H}^*\begin{bmatrix}e_x\\ e_y\\ e_z\end{bmatrix}f^*. \tag{11}$$

Selecting the operational matrix $\mathbf{H}^*$ such that

$$H_{\alpha\beta}^* = \delta_{\alpha\beta}(\nabla^2-\lambda^2)(e_2\nabla^2-\phi k)+\left[\delta_{\alpha\beta}\nabla^2-\frac{\partial^2}{\partial x_\alpha \partial x_\beta}\right][(\psi e_2-e_1)\nabla^2+\gamma-\psi\phi k]$$

$$H_{\alpha 3}^* = \frac{\partial}{\partial x_\alpha}(\nabla^2-\lambda^2)$$

$$H_{3\beta}^* = \frac{1}{\lambda^2}(e_1\nabla^2-\gamma)(\nabla^2-\lambda^2)\frac{\partial}{\partial x_\beta}$$

$$H_{33}^* = \frac{1}{\lambda^2}(\nabla^2-\lambda^2)[(1+\psi)\nabla^2-\lambda^2],$$

then eqn (10) can be reduced to

$$a_0(\nabla^2-\lambda^2)(\nabla^4-2b\nabla^2+c)f^* = -\delta(x-x_i, y-y_i), \tag{12}$$

where

$$a_0 = 1+\left(\frac{2-\nu}{1-\nu}\right)\left(\frac{G_p}{\lambda^2 D}\right)$$

$$2b = \frac{1}{a_0}\left[\left(\frac{2-\nu}{1-\nu}\right)\left(\frac{k}{\lambda^2 D}\right)+\frac{G_p}{D}\right]$$

$$c = \frac{k}{a_0 D}.$$

Using Fourier-integral transforms, in a way similar to that employed by El-Zafrany *et al.* (1994) it can be shown that

$$f^* = \sum_{k=1}^{3} a_k K_0(\lambda_k r), \tag{13}$$

where

$$\lambda_1^2, \lambda_2^2 = b \pm \sqrt{b^2 - c}, \quad \lambda_3 \equiv \lambda \tag{14}$$

and

$$a_1 = \frac{1}{2\pi a_0(\lambda_2^2-\lambda_1^2)(\lambda_3^2-\lambda_1^2)}$$

$$a_2 = \frac{1}{2\pi a_0(\lambda_1^2-\lambda_2^2)(\lambda_3^2-\lambda_2^2)}$$

$$a_3 = \frac{1}{2\pi a_0(\lambda_1^2-\lambda_3^2)(\lambda_2^2-\lambda_3^2)}. \tag{15}$$

Hence, kernel functions can be defined such that

$$\begin{bmatrix}\theta_n^* \\ \theta_t^* \\ \bar{w}^*\end{bmatrix} = \mathbf{U}\begin{bmatrix}e_x \\ e_y \\ e_z\end{bmatrix} \tag{16}$$

$$\begin{bmatrix}\bar{M}_n^* \\ M_{nt}^* \\ \bar{Q}_n^*\end{bmatrix} = \mathbf{T}\begin{bmatrix}e_x \\ e_y \\ e_z\end{bmatrix} \tag{17}$$

$$p^* = p_1 e_x + p_2 e_y + p_3 e_z, \tag{18}$$

and it can be deduced from eqns (7), (8) and (11) that

$$\mathbf{U} = \mathbf{R}\mathbf{H}^* f^* + \phi G_p \begin{bmatrix}0 & 0 & 0 \\ 0 & 0 & 0 \\ p_1 & p_2 & p_3\end{bmatrix} \tag{19}$$

and

$$\mathbf{T} = D\begin{bmatrix} \dfrac{\partial}{\partial n} & \nu\dfrac{\partial}{\partial t} & 0 \\ \dfrac{(1-\nu)}{2}\dfrac{\partial}{\partial t} & \dfrac{(1-\nu)}{2}\dfrac{\partial}{\partial n} & 0 \\ \dfrac{(1-\nu)}{2}\lambda^2 & 0 & \dfrac{(1-\nu)}{2}\lambda^2\dfrac{\partial}{\partial n} \end{bmatrix}\mathbf{R}\mathbf{H}^* f^* + G_p\begin{bmatrix} p_1 & p_2 & p_3 \\ 0 & 0 & 0 \\ \dfrac{\partial p_1}{\partial n} & \dfrac{\partial p_2}{\partial n} & \dfrac{\partial p_3}{\partial n} \end{bmatrix}, \tag{20}$$

where

$$\mathbf{R} = \begin{bmatrix} l & m & 0 \\ -m & l & 0 \\ 0 & 0 & 1 \end{bmatrix}.$$

Using eqns (6) and (11), it can also be proved that

$$p_j = \left[H^*_{3j} - \frac{\nu}{(1-\nu)\lambda^2}\left(\frac{\partial}{\partial x}H^*_{1j} + \frac{\partial}{\partial y}H^*_{2j}\right)\right]f^*, \quad j = 1,2,3,$$

which can further be reduced as follows:

$$p_\beta = -\frac{\partial}{\partial x_\beta}(\nabla^2 - \lambda^2)\left[\frac{\nu}{1-\nu}\nabla^2 + 1\right]f^*, \quad \beta = 1,2$$

$$p_3 = (\nabla^2 - \lambda^2)\left[\frac{2-\nu}{(1-\nu)\lambda^2}\nabla^2 - 1\right]f^*. \tag{21}$$

It is surprising to discover that the differential operators in eqns (21) are independent of foundation parameters, and identical to the corresponding ones for the case of thick plates on a Winkler foundation as given by El-Zafrany *et al.* (1994). The effect of the foundation on loading terms only appear in the function f^*.

By rewriting the operational matrix $\mathbf{H}^*$ as

$$\mathbf{H}^* = \mathbf{H}^*_k + \mathbf{H}^*_p,$$

where $\mathbf{H}^*_k$ is the operational matrix for the case of Winkler's foundation (El-Zafrany *et al.*, 1994), then it can be deduced that

$$\mathbf{H}^*_p = \frac{\phi G_p}{(1-\nu)}\nabla^2\begin{bmatrix} \nabla^2 - \lambda^2(1-\nu) + \dfrac{\partial^2}{\partial x^2} & \dfrac{\partial^2}{\partial x\,\partial y} & 0 \\ \dfrac{\partial^2}{\partial x\,\partial y} & \nabla^2 - \lambda^2(1-\nu) + \dfrac{\partial^2}{\partial y^2} & 0 \\ \dfrac{\nu}{\lambda^2}(\nabla^2 - \lambda^2)\dfrac{\partial}{\partial x} & \dfrac{\nu}{\lambda^2}(\nabla^2 - \lambda^2)\dfrac{\partial}{\partial y} & 0 \end{bmatrix}. \tag{22}$$

Hence, the matrices of the kernel functions $\mathbf{U}$ and $\mathbf{T}$ can be split as follows:

$$\mathbf{U} = \mathbf{U}_k + \mathbf{U}_p \tag{23}$$

$$\mathbf{T} = \mathbf{T}_k + \mathbf{T}_p, \tag{24}$$

where $\mathbf{U}_k$ and $\mathbf{T}_k$ represent the kernel functions for Winkler's case, as given by El-Zafrany

et al. (1994) and $\mathbf{U}_p$, $\mathbf{T}_p$ represent the additional effect due to the second foundation parameter G_p.

Using the previous definitions, it can be shown that

$$\mathbf{U}_p = \mathbf{R}\mathbf{H}_p^* f^* + \phi G_p \begin{bmatrix} 0 & 0 & 0 \\ 0 & 0 & 0 \\ p_1 & p_2 & p_3 \end{bmatrix} \tag{25}$$

and

$$\mathbf{T}_p = D \begin{bmatrix} \dfrac{\partial}{\partial n} & \nu \dfrac{\partial}{\partial t} & 0 \\ \dfrac{(1-\nu)}{2} \dfrac{\partial}{\partial t} & \dfrac{(1-\nu)}{2} \dfrac{\partial}{\partial n} & 0 \\ \dfrac{(1-\nu)}{2} \lambda^2 & 0 & \dfrac{(1-\nu)}{2} \lambda^2 \dfrac{\partial}{\partial n} \end{bmatrix} \mathbf{R}\mathbf{H}_p^* f^* + G_p \begin{bmatrix} p_1 & p_2 & p_3 \\ 0 & 0 & 0 \\ \dfrac{\partial p_1}{\partial n} & \dfrac{\partial p_2}{\partial n} & \dfrac{\partial p_3}{\partial n} \end{bmatrix}. \tag{26}$$

Using eqns (13) and properties of Bessel functions [see e.g. Abramowitz and Stegun (1965)], it can be shown that

$$p_j = \sum_{k=1}^{3} a_k p_j^*(\lambda_k), \quad j = 1, 2, 3 \tag{27}$$

$$\mathbf{U}_p = \sum_{k=1}^{3} a_k \mathbf{U}^{**}(\lambda_k) \tag{28}$$

$$\mathbf{T}_p = \sum_{k=1}^{3} D a_k \mathbf{T}^{**}(\lambda_k) \tag{29}$$

and explicit equations for $p_j^*(\lambda_k)$, $\mathbf{U}^{**}(\lambda_k)$ and $\mathbf{T}^{**}(\lambda_k)$ are listed in the Appendix.

REDUCTION OF DOMAIN INTEGRAL LOADING TERMS

Case of concentrated loads and moments

Consider a plate subjected to concentrated shear forces and bending moments. Let a load vector be acting at a point (x_l, y_l) and defined as

$$\vec{F} = T_x \hat{i} + T_y \hat{j} + F_z \hat{k},$$

where T_x and T_y are bending moments in the x and y directions, respectively, and F_z is a shear force in the z direction. An equivalent domain loading distribution can be obtained as follows:

$$q_l = \left(-T_x \frac{\partial}{\partial y} + T_y \frac{\partial}{\partial x} + F_z \right) \delta(x - x_l, y - y_l).$$

Hence, by using properties of Dirac delta functions (El-Zafrany, 1993), it can be shown that

$$L_j \equiv \int\int_{\Omega} p_j q_l \, dx \, dy = \left[\left(T_x \frac{\partial}{\partial y} - T_y \frac{\partial}{\partial x} + F_z \right) p_j \right] \quad \text{at} \quad (x_l, y_l). \tag{30}$$

Case of uniformly- or linearly-distributed loading

The reduction of domain integral loading terms for a case with uniformly-distributed loading can be carried out in a way similar to that demonstrated by El-Zafrany *et al.* (1994). For a case with $q(x, y)$ being a linear function of (x, y) the following redefinition of the function f^* can be employed:

$$f^* = \nabla^2 g^* + 2\pi\omega\delta(x - x_i, y - y_i) \tag{31}$$

where

$$g^* = \sum_{k=1}^{3} \frac{a_k}{\lambda_k^2} K_0(\lambda_k r)$$

and

$$\omega = \sum_{k=1}^{3} \frac{a_k}{\lambda_k^2}.$$

Hence, it can be proved that

$$L_j \equiv \int\int_{\Omega} p_j q \, dx \, dy = f_j + \oint_{\Gamma} V_j q \, d\Gamma - \oint_{\Gamma} S_j \frac{\partial q}{\partial n} \, d\Gamma, \quad j = 1, 2, 3, \tag{32}$$

where

$$f_\beta = -2\pi\omega c_i \lambda^2 \frac{\partial q}{\partial x_\beta}, \quad \beta = 1, 2$$

$$f_3 = 2\pi\omega c_i \lambda^2 q, \quad c_i \equiv \int\int_{\Omega} \delta(x - x_i, y - y_i) \, dx \, dy$$

and V_j, S_j can be expressed as

$$V_j = \sum_{k=1}^{3} a_k V_j^*(\lambda_k), \quad S_j = \sum_{k=1}^{3} a_k S_j^*(\lambda_k),$$

where explicit equations for V_j^* and S_j^* are as listed in the Appendix.

BOUNDARY INTEGRAL EQUATIONS

Using eqns (9), (16) and (17) with arbitrary values of e_x, e_y, e_z then eqn (5) can be split into the following boundary integral equations with respect to the source point (x_i, y_i):

$$c_i\theta_x(x_i, y_i) + \oint_{\Gamma} (T_{11}\theta_n + T_{21}\theta_t + T_{31}w) \, d\Gamma = \oint_{\Gamma} (U_{11}M_n + U_{21}M_{nt} + U_{31}Q_n) \, d\Gamma + L_1 \tag{33a}$$

$$c_i\theta_y(x_i, y_i) + \oint_{\Gamma} (T_{12}\theta_n + T_{22}\theta_t + T_{32}w) \, d\Gamma = \oint_{\Gamma} (U_{12}M_n + U_{22}M_{nt} + U_{32}Q_n) \, d\Gamma + L_2 \tag{33b}$$

$$c_i w(x_i, y_i) + \oint_{\Gamma} (T_{13}\theta_n + T_{23}\theta_t + T_{33}w) \, d\Gamma = \oint_{\Gamma} (U_{13}M_n + U_{23}M_{nt} + U_{33}Q_n) \, d\Gamma + L_3. \tag{33c}$$

The numerical treatment of the previous boundary integral equations can be carried

out in a way similar to that employed for linear problems [see e.g. El-Zafrany (1993)]. The boundary Γ is discretized into a number of boundary elements, and the boundary parameters $(\theta_n, \theta_t \ldots)$ are defined within each element in terms of their values at element nodes. A number of source points equal to the number of boundary nodes is initially selected so as to formulate algebraic equations in terms of unknown nodal parameters. Such source points are usually taken at a *fictitious* boundary outside the domain in order to overcome the problem of singular and divergent integrals resulting from kernel functions which have singular terms of order $\log r$, $1/r$, $1/r^2$. Different types of boundary conditions are summarized as follows.

Clamped-edge conditions

The boundary conditions for a plate with clamped edges are

$$\theta_n = \theta_t = 0, \quad w = 0. \tag{34}$$

Simply-supported edge conditions

A plate with simply-supported edges will have the following boundary conditions:

$$M_n = M_{nt} = 0, \quad w = 0. \tag{35}$$

Free-edge conditions

For the case of a plate on a Winkler foundation, the free-edge boundary conditions are

$$M_n = M_{nt} = 0, \quad Q_n = 0, \tag{36}$$

which do not consider the deformation of the foundation surface, i.e. they will lead to discontinuous deformation for the foundation surface at the free edges of the plate.

Since there is no foundation reaction beyond the plate, it can be deduced from eqn (1), for the case of a plate on a two-parameter foundation, that outside the plate the deformation of the foundation surface w_f is governed by the following differential equation:

$$G_p \nabla^2 w_f - k w_f = 0.$$

A boundary integral equation for the foundation deflection can be deduced with respect to another source point (x_i', y_i') as follows:

$$c_i' w_f(x_i', y_i') - \oint_\Gamma \left(\frac{\partial w_f^*}{\partial n}\right) w_f \, d\Gamma + \oint_\Gamma w_f^* \frac{\partial w_f}{\partial n} \, d\Gamma = 0, \tag{37}$$

where

$$w_f^* = \frac{1}{2\pi} K_0(\lambda_f r_f), \quad \lambda_f = \sqrt{k/G_p}$$

and

$$r_f = \sqrt{(x - x_i')^2 + (y - y_i')^2}.$$

At the plate boundary $w_f = w$, a shear force is generated due to the slope discontinuity of the foundation surface and is defined as follows (Selvadurai, 1979):

$$Q_n = G_p \left(\frac{\partial w_f}{\partial n} - \frac{\partial w}{\partial n}\right). \tag{38}$$

Hence, it can be deduced from eqns (38) and (4) that

$$\frac{\partial w_f}{\partial n} = \frac{Q_n}{G_p}(1+\phi G_p) - \theta_n \tag{39}$$

and eqn (37) can, therefore, be modified as follows:

$$c_i' w_f(x_i', y_i') + \oint_\Gamma \left[-w_f^* \theta_n - \left(\frac{\partial w_f^*}{\partial n}\right) w + (1+\phi G_p)\frac{w_f^*}{G_p} Q_n \right] d\Gamma = 0. \tag{40}$$

Equation (40) can numerically be analysed, simultaneously with eqns (33), with the following boundary conditions:

$$M_n = M_{nt} = 0$$

and θ_n, θ_t, w, Q_n are unknown parameters.

This approach provides explicit boundary values for Q_n, which can be employed to find the transverse shear stress at the plate edge.

NUMERICAL EXAMPLES

Boundary element computer programs based upon the theory presented in this work, and employing constant boundary elements, have been developed and tested on a PC. Validation examples with different loading and boundary conditions have been tested and their results are summarized here. All the given examples are plates made of a material with Young's modulus = 2.1×10^{11} N/m^2, and Poisson's ratio = 0.3, and with foundation parameters: $k = 6.48 \times 10^7$ N/m^3, $G_p = 0$ for Winkler cases and $G_p = 2.25 \times 10^6$ N/m for Pasternak cases.

Simply-supported rectangular plate under uniformly-distributed loading

This case represents a rectangular plate whose midplane is defined in the x–y plane in terms of the following sides: $x = 0$, $x = A$, $y = 0$, $y = B$, with $A = 1$ m, and $B = 0.5$ m. The plate was subjected to a uniformly-distributed loading of intensity $q = 6.0 \times 10^6$ N/m^2. Two values of plate thickness, with $h/A = 0.01, 0.10$, were attempted, and boundary element results were evaluated at internal nodes on the centreline: $y = B/2$. Reference displacement w_0 and moment M_0 are defined as follows:

$$w_0 = qA^4/64D, \quad M_0 = qA^2/16 \tag{41}$$

and the distributions of non-dimensional displacement and moment, w/w_0 and M_x/M_0, respectively, as obtained from boundary element analysis and analytical solutions, are shown in Figs 2 and 3, which proves that the boundary element results agree very well with corresponding analytical solutions, for the two cases of thickness.

Clamped circular plate under concentrated loading

This case and the other circular plate examples are based upon a solid disc with outer radius $r_0 = 0.5$ m. Two cases of thickness with $h/d = 0.01, 0.10$, where d is the diameter of the disc, were attempted with clamped-edge conditions, and with a concentrated force $F_z = 3.0 \times 10^6$ N acting at the plate centre. Reference parameters are defined for this case as follows:

$$w_0 = F_z r_0^2/16\pi D, \quad M_0 = F_z/4\pi. \tag{42}$$

Non-dimensional radial distributions of displacement and moment, w/w_0 and M_r/M_0, were plotted from boundary element results and corresponding analytical solutions, as demonstrated in Figs 4 and 5, respectively, which illustrate also a good agreement between boundary element results and analytical solutions.

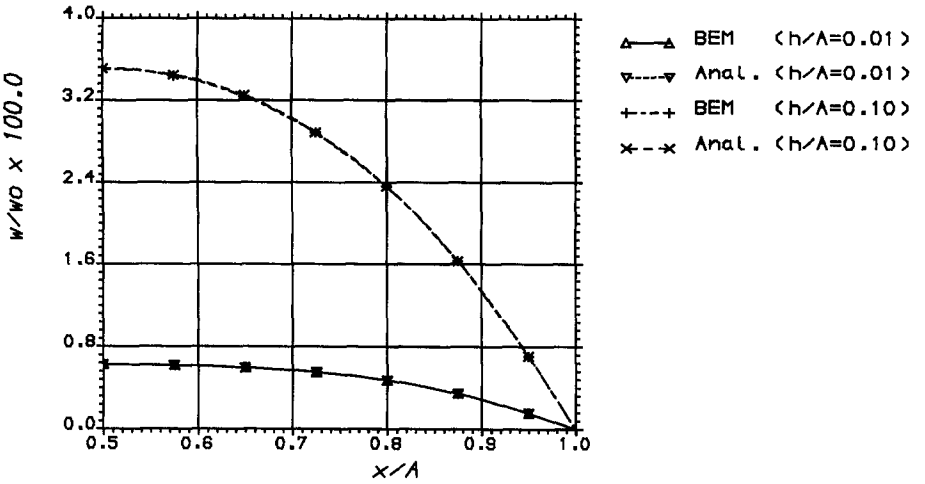

Fig. 2. Deflection of simply-supported rectangular plate under uniformly-distributed loading.

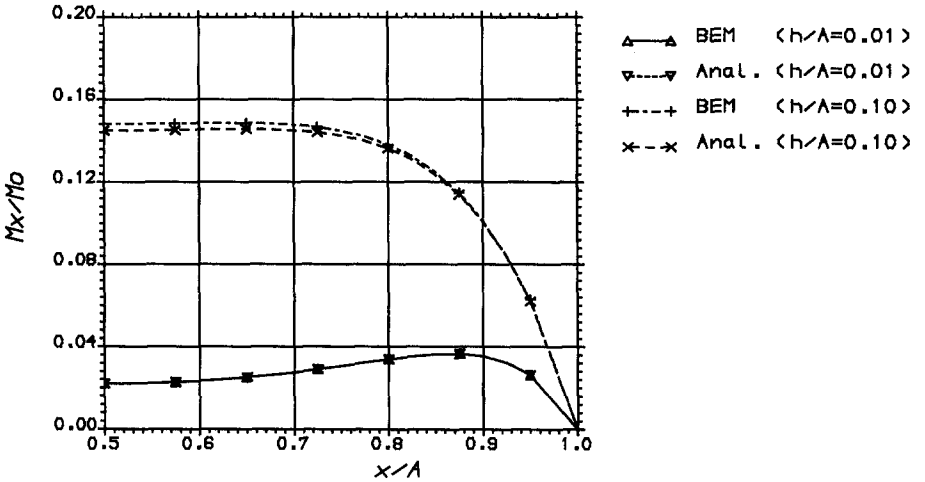

Fig. 3. Moment M_x of simply-supported rectangular plate under uniformly-distributed loading.

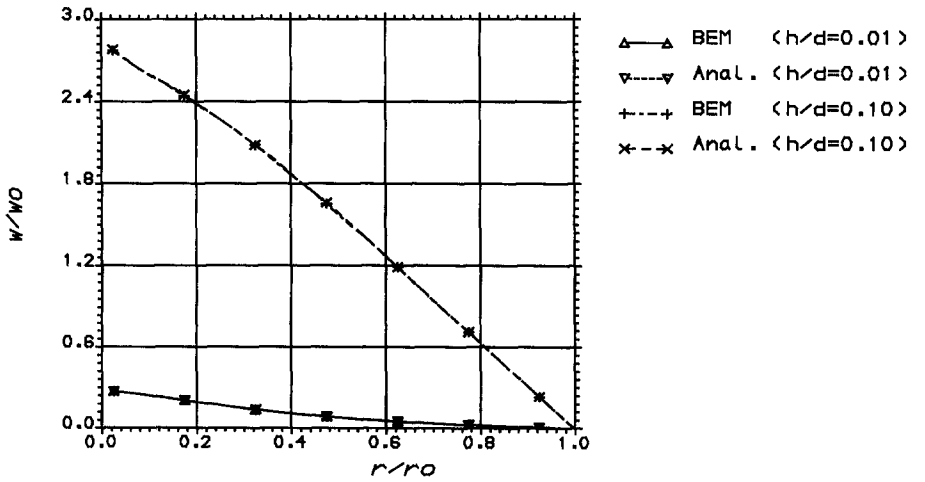

Fig. 4. Deflection of clamped circular plate under concentrated loading.

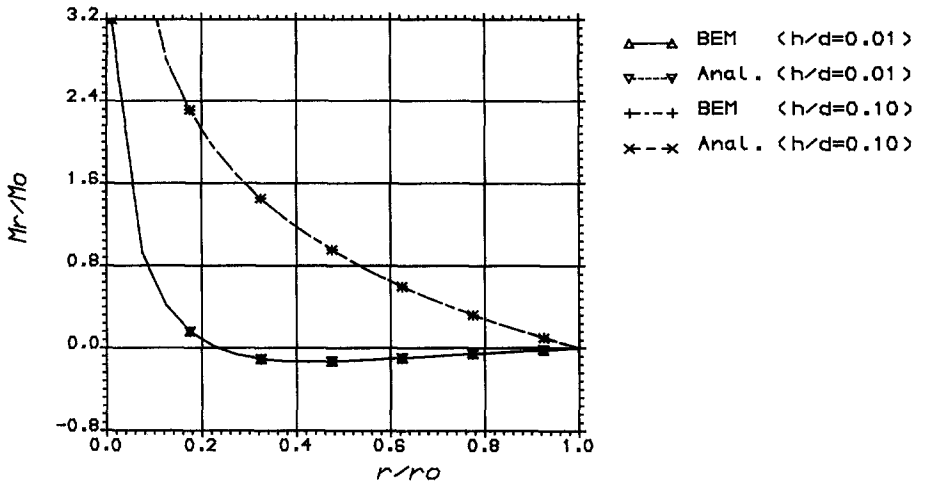

Fig. 5. Moment M_r of clamped circular plate under concentrated loading.

Free-edge circular plate under uniformly-distributed loading

Several values of thickness, ranging from $h/d = 0.01$ to 0.10, were attempted for a circular plate with free-edge conditions, and subjected to a uniformly-distributed loading with $q = 1.2 \times 10^7$ N/m^2. Two types of foundation models were attempted; a Winkler and a Pasternak foundation model, and the deflection at the outer surface of the plate is plotted against h/d, as shown in Fig. 6. It is clear from this figure that a good agreement between boundary element results and analytical solutions has been achieved for a wide range of thickness and the two types of foundation models. It is interesting to notice that the deflection of the Winkler cases has a constant value consistent with the theoretical estimation of q/k, and the Pasternak cases have a constant deflection if h/d exceeds 0.05. The radial distributions of the deflection of the plate and foundation surface, over a radial distance equal to twice the radius of the plate, is illustrated in Fig. 7, and the radial distribution of the plate internal moment M_r is demonstrated in Fig. 8. These figures confirm the excellent agreement between boundary element results and corresponding analytical solutions. It is also clear from Fig. 7 that the thicker the plate, the higher will be the discontinuity in the slope of the foundation surface, leading to a high value of the shear force per unit length Q_n generated at the plate edges. This phenomenon was confirmed by Fig. 9, which illustrates the generated edge shear force versus plate thickness. It can also be noticed from Fig. 9

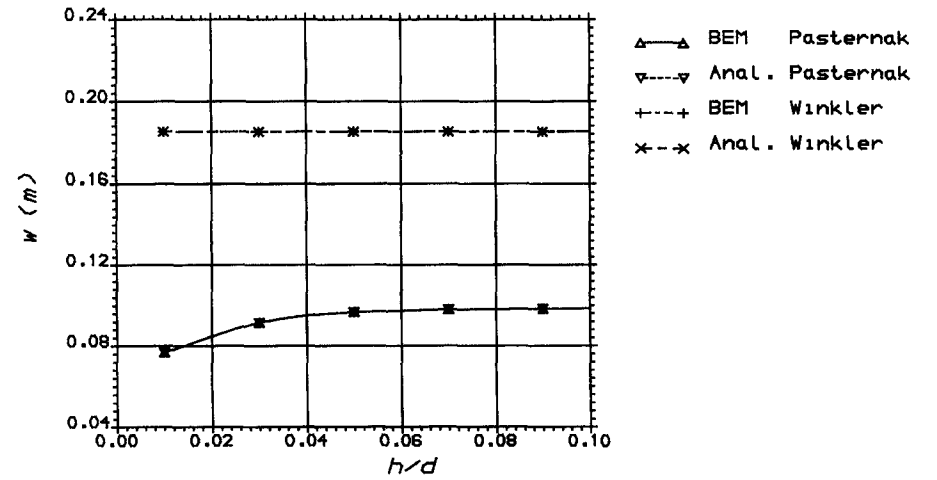

Fig. 6. Edge deflection versus plate thickness for free-edge circular plate under uniformly-distributed loading.

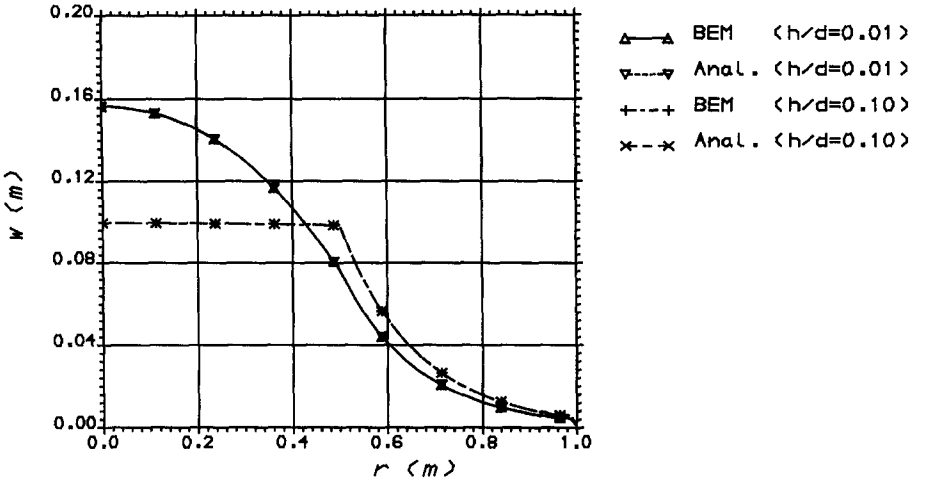

Fig. 7. Radial distribution of deflection for free-edge circular plate under uniformly-distributed loading.

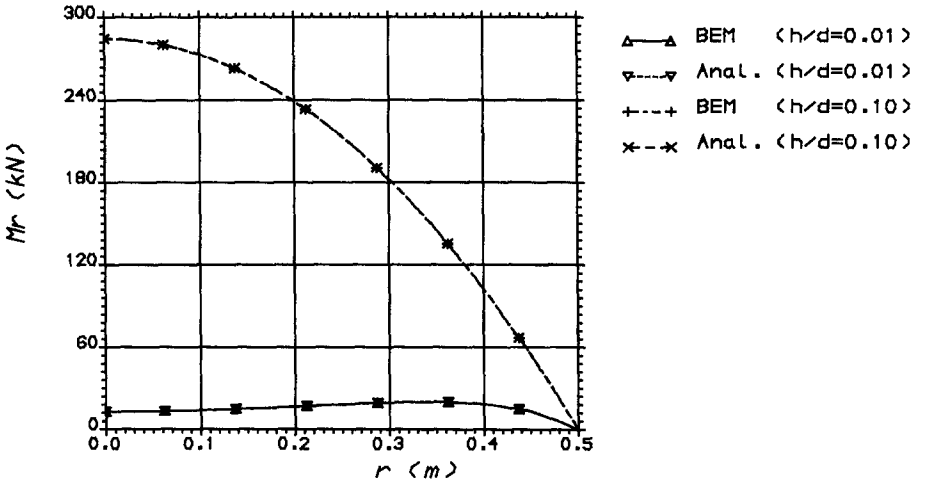

Fig. 8. Radial distribution of moment M_r for free-edge circular plate under uniformly-distributed loading.

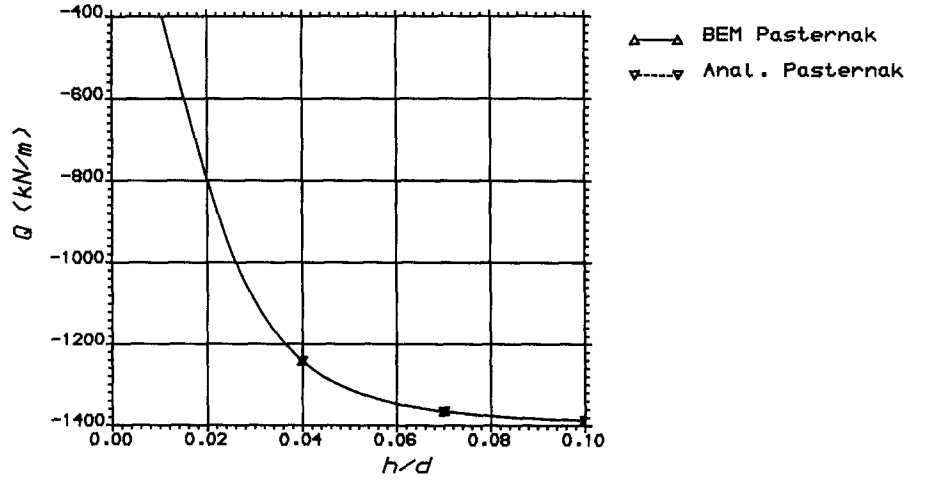

Fig. 9. Edge shear force versus plate thickness for free-edge circular plate under uniformly-distributed loading.

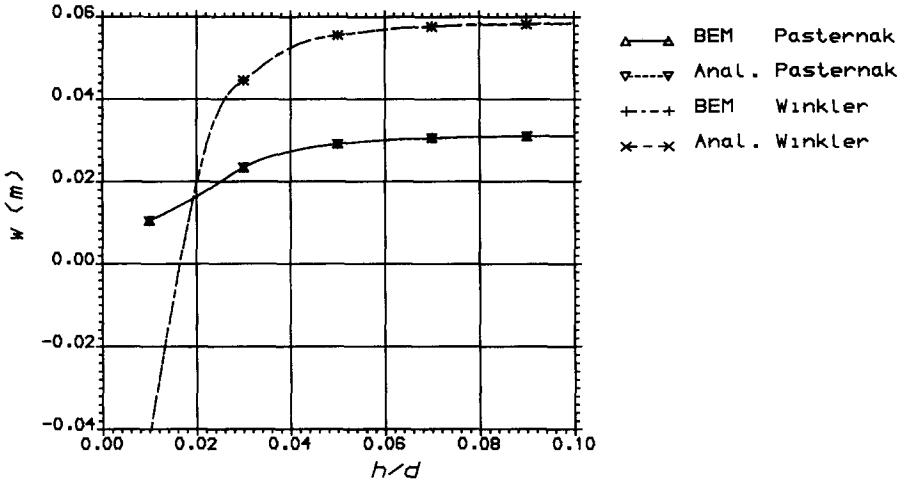

Fig. 10. Edge deflection versus plate thickness for free-edge circular plate under concentrated loading.

that Q_n reaches an asymptotic value with the increase of plate thickness, and such a value agrees with that obtained from the following analytical expression:

$$(Q_n)_{\text{asym.}} = G_p \frac{dw_f}{dr} = -G_p w(r_0) \lambda_f \frac{K_1(\lambda_f r_0)}{K_0(\lambda_f r_0)}. \tag{43}$$

Free-edge circular plate under concentrated loading

This is similar to the previous case but the plate is subjected to a shear force $F_z = 3.0 \times 10^6$ N acting at its centre. Boundary element results were plotted together with corresponding analytical solutions, as shown in Figs 10, 11 and 12, which display observations similar to those deduced for the corresponding figures of the previous case. It can also be seen that thick plates under a concentrated loading will have a uniform distribution of deflection similar to that obtained for a case with a uniformly-distributed loading with $q = F_z/\pi r_0^2$. This phenomenon agrees with the concept of rigid plates discussed by Vlasov and Leont'ev (1966). The edge shear force Q_n reaches also an asymptotic value in agreement with that obtained from eqn (43), as can be seen in Fig. 12.

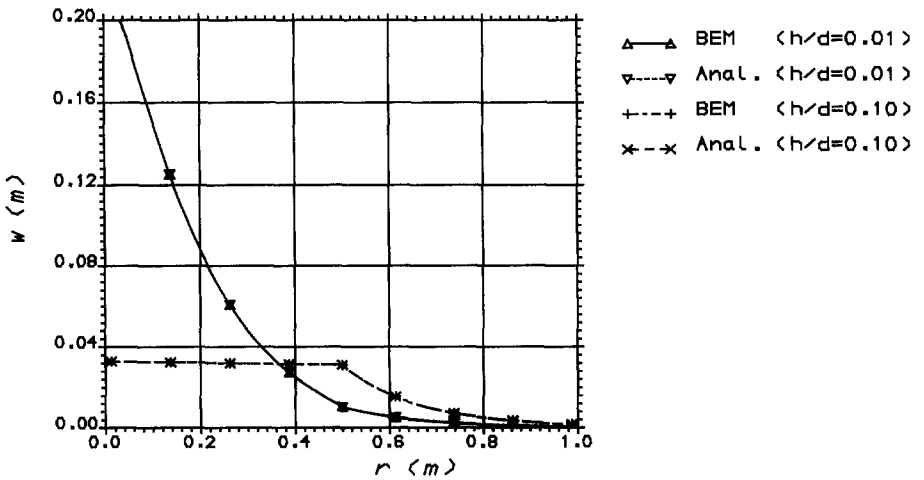

Fig. 11. Radial distribution of deflection for free-edge circular plate under concentrated loading.

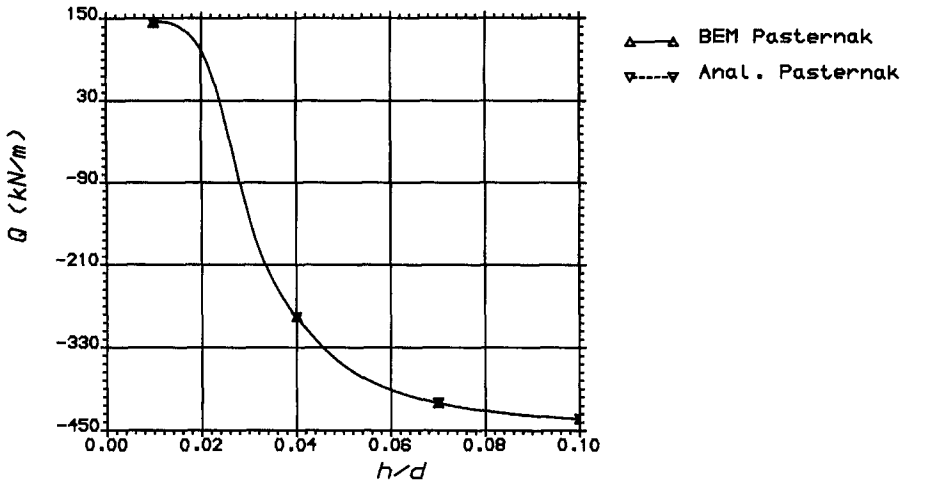

Fig. 12. Edge shear force versus plate thickness for free-edge circular plate under concentrated loading.

Free-edge rhombic plate under symmetric loading

This case has been suggested to test the behaviour and convergence of boundary element solutions for cases with singular corner loading. It is based upon a free-edge plate with a rhombic midplane *abcd*, as shown in Fig. 13, resting on a Pasternak elastic foundation, and having material and foundation properties similar to previous cases.

A *rigid* case was tested first, with the rhombic plate subjected to a uniformly-distributed loading of intensity $q = 5.0 \times 10^6$ N/m^2. The rigidity was induced by selecting a high value for the plate thickness ($h = 0.5$ m), and the boundary element analysis has yielded a uniform deflection $w \approx 0.0404$ m. Several other cases, with different values of thickness and subjected to concentrated shear forces acting at the cornes a, b, c and d, each of value

$$F = qA/4,$$

where A is the midplane area, were tested. The deflection distribution along the longer diagonal (the x-axis) was plotted for different cases attempted, as shown in Fig. 14. It is clear from this figure that with the increase of plate thickness the deflection of the rhombic plate under corner forces is converging towards the uniform deflection obtained for the rigid case under equivalent uniformly-distributed loading. Although the corner forces have generated additional corner singularity, making it numerically impossible to find the solution at plate corners, the use of non-conforming constant boundary elements has resulted in an automatic elimination of corner problems in boundary integral equations, leading to accurate BEM solutions elsewhere.

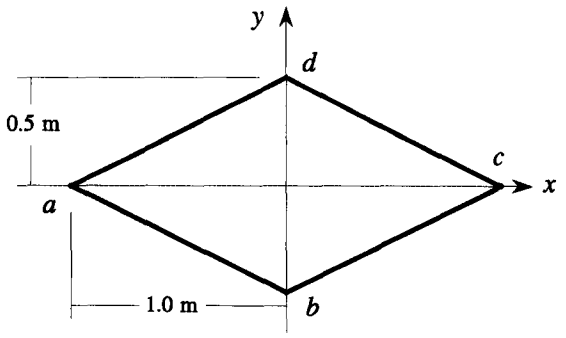

Fig. 13. Midplane of rhombic plate.

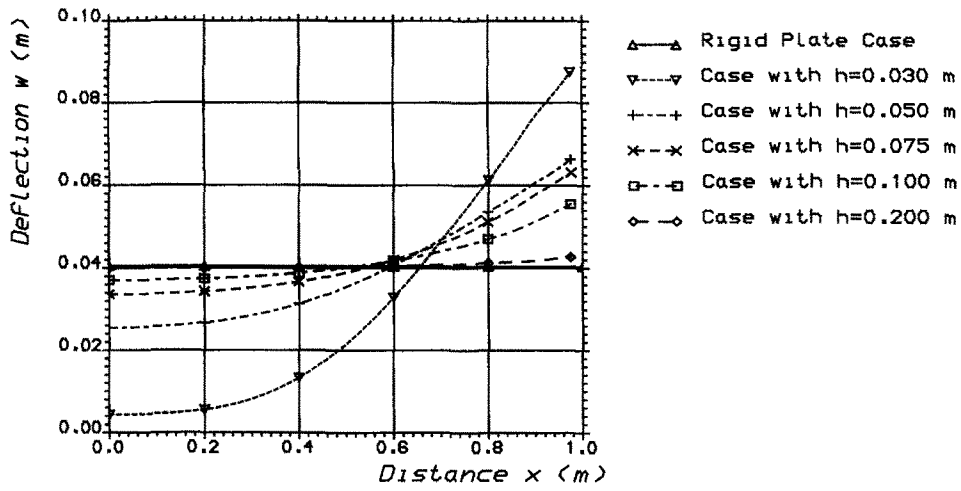

Fig. 14. Deflection of free-edge rhombic plate resting on a Pasternak foundation.

CONCLUSIONS

It is clear from the previous applications that the boundary element formulations presented in this work have led to an accurate analysis for plates with different boundary and loading conditions resting on one- or two-parameter elastic foundations. Boundary element results of the examples with free-edge conditions were in an excellent agreement with corresponding analytical solutions, and they also confirm the advantages of two-parameter foundation models, which lead to practically acceptable results for such cases. The use of fictitious boundaries to overcome divergent integral problems has performed well for plate shapes usually employed in foundation problems, including rhombic or skew plates.

REFERENCES

Abramowitz, M. and Stegun, I. A. (1965). *Handbook of Mathematical Functions*. Dover Publications, New York.

Balaš, J., Sládek, V. and Sládek, J. (1984). The boundary integral equation method for plates resting on a two-parameter foundation. *ZAMM* **64**, 137–146.

El-Zafrany, A. (1993). *Techniques of the Boundary Element Method*. Ellis Horwood, Chichester.

El-Zafrany, A., Fadhil, S. and Al-Hosani, K. (1994). Boundary element analysis of thick Reissner plates resting on Winkler foundation. Submitted to *Int. J. Numer. Meth. Engng*.

Jianguo, W., Xiuxi, W. and Maokuang, H. (1992). Fundamental solution and boundary integral equations for Reissner's plates on two parameter foundations. *Int. J. Solids Structures* **29**, 1233–1239.

Katsikadelis, J. T. and Kallivokas, L. F. (1986). Clamped plates on Pasternak-type elastic foundation by the boundary element method. *ASME J. Appl. Mech.* **53**, 909–917.

Puttonen, J. and Varpasuo, P. (1986). Boundary element analysis of plates on elastic foundations. *Int. J. Numer. Meth. Engng* **23**, 287–303.

Reissner, E. (1945). The effect of transverse shear deformation on the bending of elastic plates. *ASME J. Appl. Mech.* **12**, A69–A77.

Selvadurai, A. P. S. (1979). *Elastic Analysis of Soil–Foundation Interaction*. Elsevier Science, Amsterdam.

Vlasov, V. Z. and Leont'ev, N. N. (1966). Beams, plates and shells on elastic foundation. U.S. Department of Commerce, Springfield, VA.

APPENDIX

Domain loading functions

$$p^*_\beta(\lambda_k) = \lambda_k(\lambda_k^2 - \lambda^2)\left[\left(\frac{\nu}{1-\nu}\right)\frac{\lambda_k^2}{\lambda^2} + 1\right]\frac{\partial r}{\partial x_\beta}K_1(z)$$

$$p^*_3(\lambda_k) = (\lambda_k^2 - \lambda^2)\left[\left(\frac{2-\nu}{1-\nu}\right)\frac{\lambda_k^2}{\lambda^2} - 1\right]K_0(z).$$

Kernel functions for a second foundation parameter

$$U^{**}_{\alpha\beta}(\lambda_k) = \phi G_p\left\{(\hat{n}_\alpha \cdot \hat{i}_\beta)[c_3K_0(z) + c_4B_1(z)] - c_4\frac{\partial r}{\partial n_\alpha}\frac{\partial r}{\partial x_\beta}A_1(z)\right\}$$

$$U^{**}_{\alpha 3}(\lambda_k) = 0$$

$$U^{**}_{3\beta}(\lambda_k) = \phi G_p \lambda_k (\lambda_k^2 - \lambda^2) \frac{\partial r}{\partial x_\beta} K_1(z)$$

$$U^{**}_{33}(\lambda_k) = \phi G_p (\lambda_k^2 - \lambda^2) \left[\left(\frac{2-\nu}{1-\nu} \right) \frac{\lambda_k^2}{\lambda^2} - 1 \right] K_0(z)$$

$$T^{**}_{1\beta}(\lambda_k) = \phi G_p \lambda_k \left\{ - \left[l_\beta \frac{\partial r}{\partial n} + \nu (\hat{i} \cdot \hat{i}_\beta) \frac{\partial r}{\partial t} \right] F^{**}(z) + c_4 \frac{\partial r}{\partial x_\beta} \left[g K_1(z) + (4g - 1 - \nu) \right] \frac{A_1(z)}{z} \right\} + \frac{G_p}{D} p^*_\beta(\lambda_k)$$

$$T^{**}_{2\beta}(\lambda_k) = \phi G_p \lambda_k (1-\nu) \left\{ c_4 \frac{\partial r}{\partial n} \frac{\partial r}{\partial t} \frac{\partial r}{\partial x_\beta} \left[K_1(z) + 4 \frac{A_1(z)}{z} \right] - \frac{1}{2} \left[l_\beta \frac{\partial r}{\partial t} + (\hat{i} \cdot \hat{i}_\beta) \frac{\partial r}{\partial n} \right] F^{**}(z) \right\}$$

$$T^{**}_{13}(\lambda_k) = \frac{G_p}{D} p^*_3(\lambda_k)$$

$$T^{**}_{23}(\lambda_k) = 0$$

$$T^{**}_{3\beta}(\lambda_k) = \frac{G_p}{D} \left\{ l_\beta \left[c_3 K_0(z) + c_4 K_1(z) + c_5 \frac{K_1(z)}{z} \right] - (c_4 + c_5) \frac{\partial r}{\partial n} \frac{\partial r}{\partial x_\beta} A_1(z) \right\}$$

$$T^{**}_{33}(\lambda_k) = -\tfrac{1}{2} \phi G_p \lambda_k (\lambda_k^2 - \lambda^2) [(4-\nu)\lambda_k^2 - (1-\nu)\lambda^2] \frac{\partial r}{\partial n} K_1(z),$$

where

$$\alpha = 1,2, \quad \beta = 1,2, \quad (l_1, l_2) \equiv (l, m), \quad (\hat{i}_1, \hat{i}_2) \equiv (\hat{i}, \hat{j})$$

$$\hat{n} \equiv \hat{n}_1 = l\hat{i} + m\hat{j}, \quad \hat{t} \equiv \hat{n}_2 = -m\hat{i} + l\hat{j}$$

$$z = \lambda_k r, \quad r = \sqrt{(x - x_i)^2 + (y - y_i)^2}$$

$$c_3 = \lambda_k^2 (\lambda_k^2 - \lambda^2), \quad c_4 = \frac{\lambda_k^4}{(1-\nu)}$$

$$c_5 = c_3 \left[\frac{\lambda_k^2}{(1-\nu)\lambda^2} + 1 \right]$$

$$A_1(z) = K_0(z) + \frac{2K_1(z)}{z}$$

$$B_1(z) = K_0(z) + \frac{K_1(z)}{z}$$

$$F^{**}(z) = (c_3 + c_4) K_1(z) + 2c_4 \frac{A_1(z)}{z}$$

$$g = \left(\frac{\partial r}{\partial x} \right)^2 + \nu \left(\frac{\partial r}{\partial y} \right)^2.$$

Domain loading boundary kernel functions

$$V^*_\beta(\lambda_k) = (\lambda_k^2 - \lambda^2) \left[\left(\frac{\nu}{1-\nu} \right) \frac{\lambda_k^2}{\lambda^2} + 1 \right] \left[(\hat{n} \cdot \hat{i}_\beta) \frac{K_1(z)}{z} - \frac{\partial r}{\partial n} \frac{\partial r}{\partial x_\beta} A_1(z) \right]$$

$$V^*_3(\lambda_k) = -\frac{1}{\lambda_k} (\lambda_k^2 - \lambda^2) \left[\left(\frac{2-\nu}{1-\nu} \right) \frac{\lambda_k^2}{\lambda^2} - 1 \right] \frac{\partial r}{\partial n} K_1(z)$$

$$S^*_\beta(\lambda_k) = \frac{1}{\lambda_k} (\lambda_k^2 - \lambda^2) \left[\left(\frac{\nu}{1-\nu} \right) \frac{\lambda_k^2}{\lambda^2} + 1 \right] \frac{\partial r}{\partial x_\beta} K_1(z)$$

$$S^*_3(\lambda_k) = \frac{1}{\lambda_k^2} (\lambda_k^2 - \lambda^2) \left[\left(\frac{2-\nu}{1-\nu} \right) \frac{\lambda_k^2}{\lambda^2} - 1 \right] K_0(z).$$